Journal of Colloid and Interface Science 513 (2018) 911–922

Contents lists available at ScienceDirect

Journal of Colloid and Interface Science

journal homepage: www.elsevier.com/locate/jcis

Feature Article

Tailoring the self-assembly of linear alkyl chains for the design of advanced materials with technological applications

Cristina E. Hoppe *, Roberto J.J. Williams *

Institute of Materials Science and Technology (INTEMA), University of Mar del Plata and National Research Council (CONICET), Av. J. B. Justo 4302, 7600 Mar del Plata, Argentina

GRAPHICAL ABSTRACT

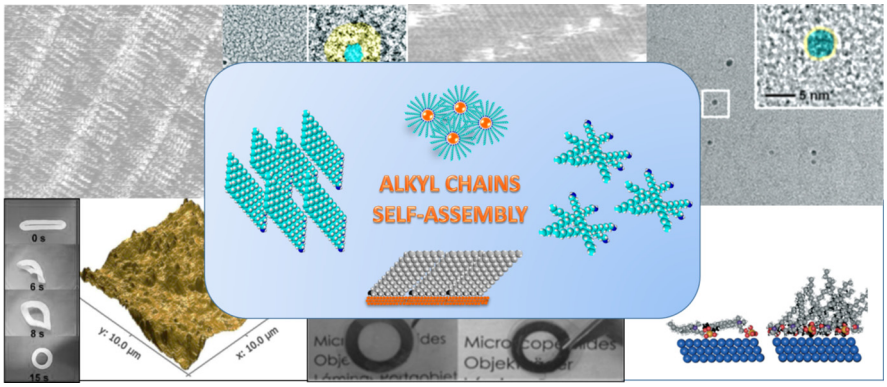

ARTICLE INFO

Article history:
Received 30 August 2017
Revised 11 October 2017
Accepted 12 October 2017
Available online 13 October 2017

Keywords:
Alkyl chains
Amphiphilic materials
Crystallization of alkyl chains
self-assembled monolayers (SAMs)
Self-assembly of alkyl chains

ABSTRACT

The self-assembly of *n*-alkyl chains at the bulk or at the interface of different types of materials and substrates has been extensively studied in the past. The packing of alkyl chains is driven by Van der Waals interactions and can generate crystalline or disordered domains, at the bulk of the material, or self-assembled monolayers at an interface. This natural property of alkyl chains has been employed in recent years to develop a new generation of materials for technological applications. These studies are dispersed in a variety of journals. The purpose of this article was to discuss some selected examples where these advanced properties arise from a process involving the self-assembly of alkyl chains. We included a description of electronic devices and new-generation catalysts with properties derived from a controlled two-dimensional (2D) or three-dimensional (3D) self-assembly of alkyl chains at an interface. Then, we showed that controlling the crystallization of alkyl chains at the bulk can be used to generate a variety of advanced materials such as superhydrophobic coatings, shape memory hydrogels, hot-melt adhesives, thermally reversible light scattering (TRLS) films for intelligent windows and form-stable phase change materials (FS-PCMs) for the storage of thermal energy. Finally, we discussed two examples where advanced properties derive from the formation of disordered domains by physical association of alkyl chains. This was the case of photoluminescent nanocomposites and materials used for reversible optical storage.

* Corresponding authors.
E-mail addresses: hoppe@fi.mdp.edu.ar (C.E. Hoppe), williams@fi.mdp.edu.ar (R.J.J. Williams).

https://doi.org/10.1016/j.jcis.2017.10.048
0021-9797/

Contents

1. Introduction

The self-assembly of *n*-alkyl chains at the bulk or at the interface of different types of materials and substrates has been extensively studied. The packing of these chains arises from Van der Waals interactions and can generate either crystalline domains involving fractions of alkyl chains packed in an *all trans* conformations or amorphous aggregates. Examples of cases that have been deeply investigated are self-assembled monolayers (SAMs) [1,2] and crystalline domains produced in comb-like polymers with pendant alkyl chains [3,4].

SAMs are formed by spontaneous adsorption of organic molecules on the surface of a substrate. In SAMs of molecules containing long alkyl chains, interactions between the head group and the substrate, as well as van der Waals interactions between adjacent adsorbed molecules, play a fundamental role in determining attachment, orientation and packing density of the final structure [1]. Influence of size related parameters, like van der Waals radii of the head and tail groups and lattice parameters of the substrate, on the degree of order and orientation of the monolayer have been extensively studied [2]. Commonly, structural disorder or defects appear when differences between the sizes of head and tail groups and/or between the size of these groups and the lattice parameter of the substrate increase. In general, the tendency of the alkyl chains to maximize interactions between -CH_2 groups produces well-arranged, densely packed monolayers perpendicular to the surface. However, if the substrate has a chemical structure enabling the adsorption of these groups, like a graphene surface, alkyl chains can lay parallel to the surface forming a 2D SAM [5]. SAMs of alkyl chains can also be formed on curved surfaces, like those present in nanoparticles (NPs), with alkyl molecules bearing functional groups chemically compatible with the surface (e.g., thiols or amines in the case of noble metals). Besides controlling internal order and structure of the monolayer, van der Waals interactions between alkyl chains are also responsible for the arrangement of NPs in different crystalline structures or assemblies (body-centered cubic, bcc, face-centered cubic, fcc, hexagonal close packed, hcp or lower symmetry arrays) called "superlattices" or "crystals of nanocrystals" [6–8]. As alkyl chains have a high tendency to form densely packed arrangements that fill the space around the particles, the preferred structure adopted in each case will depend on the length of the alkyl chain and the size of the NPs core [6]. A high level of chain interdigitation is characteristic of these structures, with packing densities so high that can be compared with those found in solid crystalline alkane phases [6].

Comb-like polymers are characterized by the presence of long side chains joined to a main polymer backbone through chemical junctions (also called attachment bridges) [3]. Due to the spatial restriction imposed by the presence of the polymer backbone, a high level of interaction between side chains is expected in this kind of configuration. When side chains are linear alkyl groups, the structure and properties of these polymers are determined by the tendency of alkyl side chains to close packing. However, limitations are expected that depend on the flexibility, regularity and physicochemical properties of the main polymer chain and the attachment bridges. These are characteristics that strongly control their relaxation transitions, their ability to crystallize (also their crystal structure) and their potential to form superstructures and gels [3]. Long alkyl groups tend to aggregate through a process of "nanophase separation" to form domains with typical dimensions in the range 5–20 Å [9]. Hence, materials with very diverse properties can be obtained by controlling the structure of the polymer backbone and the side chains [10]. Some well-studied examples of comb-like polymers containing alkyl chains can be found in the synthesis of poly(α-olefins), poly(*n*-alkyl acrylates), poly (viny-*n*-alkyl) esters, etc.

Other well-studied examples of structures formed by the self-assembly of alkyl chains are those of metallic thiolates [11] and siloxane–organic hybrids from amphiphilic silicon-based precursors [12].

Besides the vast literature of fundamental studies dealing with the characterization of self-assemblies of alkyl chains, there is a set of other studies showing that tailoring the packing of alkyl chains can be used to generate advanced materials with technological applications. These reports are classified under different headings and dispersed in a large variety of journals from different fields. Based on the final application, a variety of examples can be found that range from the tuning of gene transfer properties of cationic lipids [13] to the super-gelation and emissive properties of star-shaped stilbene derivatives [14]. Same type of hydrophobic interactions can conduct, using a completely different chemistry and synthetic strategy, to the design of shape memory polymers [15] or artificial light-harvesting materials [16]. Hence, a comprehensive reading of the literature clearly shows that the strong tendency of alkyl chains to suffer self-assembly processes can be used for the design of new functional materials with applications in a large variety of fields. The aim of this feature article is to discuss just a selection of these studies to demonstrate that the self-assembly of alkyl chains is an extraordinary tool for the design of advanced materials. Selected examples begin with two cases

employing SAMs for applications in electronic devices and as novel catalysts. Then, several examples based on crystalline aggregates in the bulk are discussed, including superhydrophobic materials, shape memory hydrogels with high mechanical strength and self-healing ability, hot-melt adhesives, thermally-reversible light scattering (TRLS) films and materials for thermal energy storage (FS-PCMs). Finally, examples based on the formation of amorphous aggregates of alkyl chains are presented. These include materials with reversible optical storage and photoluminescent nanocomposites.

2. Advanced materials based on SAMs of alkyl chains

Formation of SAMs of alkyl chains on flat substrates or nanostructures can be used for controlling wettability, reactivity, assembly capacity or even electronic properties of materials. Most common examples can be found in the functionalization of metal and carbon nanostructures with alkylthiols or alkylamines to confer them dispersability in non-polar solvents [17], capacity to form colloidal crystals by self-assembly [18] or interesting tribological and super-wettability properties [19]. In this section, we will limit the discussion to two recent examples showing that this kind of functionalization can lead to even less expected effects, like tuning of electronic and catalytic properties of materials.

2.1. Graphene field-effect devices

There is an outstanding interest for the use of graphene in electronic applications. This requires tailoring the charge carrier density and location of the work function, issues that can be modulated by p-type or *n*-type doping [20]. One way to produce the desired doping is by physical adsorption of molecules with charge transfer capacity to the graphene surface. In this case, the main problem is the precise control of the density of the adsorbate at the surface. An elegant answer to this requirement was recently proposed based on the 2D self-assembly of alkyl chains at the graphene surface [5]. Two *n*-alkyl amines with different lengths were selected as adsorbates: octadecylamine (ODA, 18 carbon atoms) and nonacosylamine (NCA, 29 carbon atoms). They provide *n*-type doping by the amine groups.

Fig. 1 shows self-assembled layers of ODA and NCA over highly ordered pyrolitic graphite used as a model surface. Alkyl chains adsorb parallel to the surface due to the commensurability between the adsorbate and the substrate lattice. For ODA, a characteristic tail-to-tail (or head-to-head) pattern is observed, facilitating the H-bonds among amine groups. For NCA, tail-to tail self-assembled patterns alternate with tail-to-head ones. This arises from the higher intermolecular and molecule-substrate interactions for the longer alkyl amine that produces a kinetic trapping of the less stable pattern. However, in both cases the density of amine groups at the graphitic surface could be precisely controlled by the self-assembly of alkyl chains (either tail-to-tail or tail-to head) in domains covering the whole surface.

The doping with both alkyl amines was also performed on graphene grown by chemical vapor deposition (CVD). Using Raman spectroscopy it was found that the charge carrier concentration was 1.59 times higher with ODA than with NCA. This agrees with the length ratio (1.6) between NCA and ODA and confirms that the density of adsorbed amine groups, which depends on the length of the self-assembled alkyl amines, can control the doping.

The effect of doping by both alkyl amines was also assessed by electrical measurements of four-probe back gated graphene field-effect transistors. It was observed that the amount of electrons injected in the device functionalized with ODA was 1.52 times higher than in the device functionalized with NCA. Again, this ratio is close to the density ratio of amine groups on the surface between both adsorbates (1.6) and reassures the fact that doping can be controlled by the self-assembly of alkyl amines at the graphene surface.

2.2. Catalytic response of a new generation of Pd-based hydrogenation catalysts

A new generation of industrial hydrogenation catalysts based on supported Pd, Pt, and Pd–Pt NPs employs hexadecyl-2-hydroxye thyldimethyl ammonium dihydrogen phosphate (HHDMA, Fig. 2) in a colloidal aqueous solution. HHDMA acts as a reducing agent of Pd or Pt salts and as a stabilizing ligand of the metallic NPs [21,22].

The relative amount of HHDMA has a significant influence on the activity and selectivity of these new catalysts. The reason of this behavior was recently investigated by comparing the structure

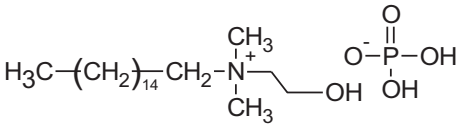

Fig. 2. Chemical structure of HHDMA.

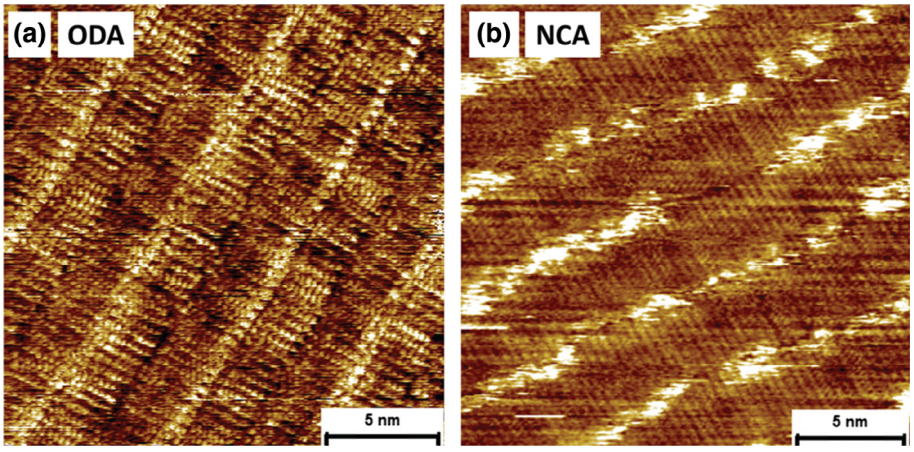

Fig. 1. STM images showing self-assembled layers of ODA and NCA over a highly ordered pyrolitic graphite (HOPG) surface. Reprinted with permission from Phillipson et al. [5].

and catalytic behavior of a series of Pd-HHDMA catalysts supported on titanium silicate ($TiSi_2O_6$) [23].

The series of synthesized catalysts contained the same metal concentration (0.3 wt%) and average size of Pd NPs (5 nm) but different HHDMA contents varying from 0.3 to 16.8 wt%. Tests showed an increased catalytic activity in hydrogenation reactions when increasing the amount of HHDMA. This is a rather counterintuitive observation because it could be expected that an increase in the amount of stabilizing ligands would decrease the accessibility to the metallic surface with a corresponding decrease of the activity. The explanation of this peculiar behavior was obtained from transmission electron microscopy (TEM) observations and theoretical predictions of the ordering of the long alkyl chains of HHDMA employing Density Functional Theory (DFT) calculations.

Fig. 3 shows TEM images of colloidal Pd NPs (core) with the layer of stabilizing ligands (shell). The amount of HHDMA increases from (a) to (c). The most relevant feature observed in the micrographs is the increase in the thickness of the shell when increasing the amount of HHDMA. This must be related to the orientation of the alkyl chains of HHDMA at the surface of Pd NPs (Fig. 4).

For a low concentration of HHDMA, alkyl chains are flattened on the Pd surface in agreement with the small thickness of the shell observed in TEM images. At high HHDMA concentrations, alkyl chains self-assemble as extended chains packed in a monolayer (SAM). This explains the large shell thickness shown by TEM images. The different arrangement of alkyl chains explains the observed increase in catalytic activity when increasing the HHDMA concentration. When the alkyl chains extend horizontally on the surface, they have the maximum capacity of blocking catalytic Pd active sites. On the other hand, increasing the HDDMA concentration has two opposite effects: there is a larger fraction of Pd sites directly blocked by the head of the ligand but, at the same time, Pd sites indirectly blocked by the alkyl chains decreased. The last effect seems to be the prevailing one.

3. Advanced materials based on the crystallization of alkyl chains in the bulk

The existence of small crystalline regions in the bulk of materials has significant effects on their properties that can be useful in the design of specific functions. Crystals can be used as thermoreversible crosslinking points, mechanical reinforcing structures, tortuosity elements, light scattering domains, etc. Considering these effects, several strategies have been proposed, based on the crystallization of alkyl chains, for the synthesis of superhydrophobic materials [24,25], hydro- and organogels [26,27], phase change materials (PCMs) [28], shape memory polymers [29,30], TRLS films [31], hot-melt adhesives [32], among others. Some selected examples are discussed in the following sections.

3.1. Superhydrophobic materials

Significant efforts have been dedicated in the last decades to the development of superhydrophobic materials employing a variety of chemistries ([25] and references therein). A material with outstanding properties was developed entirely based on the crystallization of alkyl chains [25]. Silica NPs were grafted with octadecyl chains by reacting octadecylisocyanate with the silanol (SiOH) groups present at the surface, in a single step (18 h at 80 °C). After filtration, washing and drying, a powder composed of grafted silica NPs was obtained. It was processed as a colloidal solution in xylene that was dropped over a substrate and heated at 150 °C to obtain a coating.

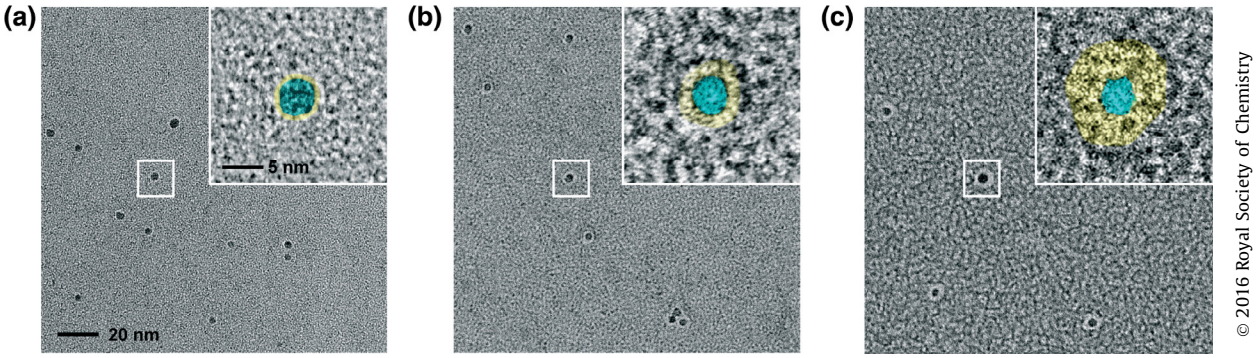

Fig. 3. TEM images of the colloidal Pd NPs (core) with the layer of stabilizing ligands (shell). The amount of HHDMA increases from (a) to (c). Reprinted with permission from Albani et al. [23].

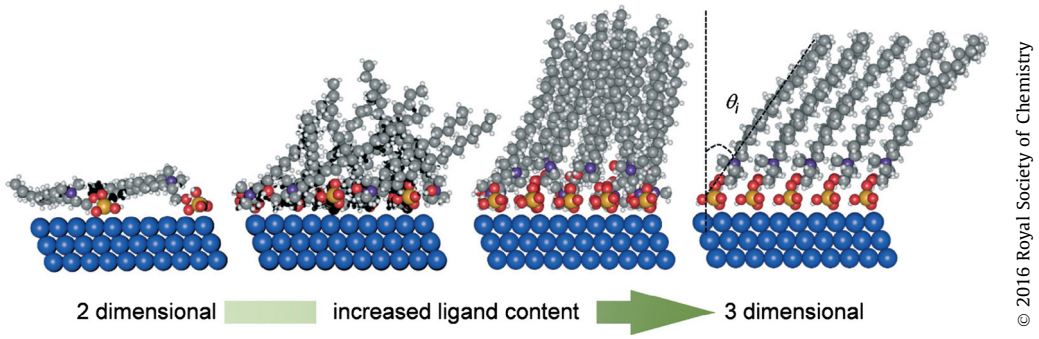

Fig. 4. Orientation of the alkyl chains of HHDMA at the surface of Pd, predicted by DFT calculations. Reprinted with permission from Albani et al. [23].

Physical crosslinking of silica NPs was produced by the crystallization of octadecyl chains. The melting temperature was 120 °C and the material could be re-processed or healed above this temperature. The static water contact angle (WCA) of the coating was 166 ± 1°, with a sliding angle close to 6°. WCA values were higher than 155 ° in a range of pH values comprised between 1 and 13. Therefore, a very simple chemistry gave place to an outstanding superhydrophobic material.

The superhydrophobicity is usually the result of two different factors: the intrinsic hydrophobicity of the material derived from its chemical structure and the dual (micro-nano) scale roughness of its surface. In order to separate both effects, the material was subjected to a very high static pressure to reduce the surface roughness to about 10 nm, removing the influence of the second factor. This led to a WCA value of 106°. Hence, the very high WCA value observed for the as-processed material derives from its particular surface rugosity (average roughness of 70 nm, Fig. 5).

The surface rugosity is possibly the result of the restrictions of the size and shape of crystals imposed by the anchoring of the alkyl chains to the silica NPs. Fracturing the material and measuring WCA at the new produced surfaces gave the same high values. This indirectly confirms that rugosity derives from the size and shape of crystals formed both at the surface and at the bulk of the material. This is an extremely important property that enabled to keep superhydrophobicity after severely abrading or rubbing the surface.

3.2. Shape memory hydrogels with high mechanical strength and self-healing ability

Shape memory polymers are used in different applications for their capacity to restore an initial shape by application of a convenient stimulus. In particular, the family of hydrogels (polymer networks containing a large fraction of water) have drawn considerable interest for biomedical applications due to their compatibility with biological tissues. An important sub-family of hydrogels bases its shape-memory properties on the crystallization of alkyl chains in the bulk [27,33,34]. One of the examples described in Ref. [27] will be briefly described to show the effect of alkyl chains associations on shape memory properties.

Hydrogels were synthesized by free-radical copolymerization of a highly hydrophilic monomer, acrylic acid (AAc, 50 mol %), with a hydrophobic monomer, *n*-octadecylacrylate (ODA, 50 mol %) that supplies the long (C18) alkyl chains. The reaction was carried out in a micellar aqueous solution containing sodium dodecyl sulphate (SDS) as surfactant. ODA was present in the micelles stabilized by SDS and this enabled to produce a multiblock structure of the copolymer (e.g. a large fraction of the alkyl chains was present in neighbouring segments). In a final step the surfactant was removed from the hydrogel (different properties were generated before removing the surfactant [27]).

The hydrogel contained 64 % water and exhibited crystalline domains produced by the tail-to tail self-assembly of alkyl chains. The melting temperature was 51 °C and crystallization was observed at 44 °C. From the experimental value of the melting heat it was inferred that 56 % of methylene groups of octadecyl chains were crystallized. This gave the hydrogel a high mechanical strength at room temperature. The storage modulus dropped from 8.4 MPa at 25 °C (strong gel) to 7.5 kPa at 65 °C (weak gel), in a completely reversible way. Of most importance for shape memory properties is the fact that amorphous aggregates of alkyl chains, present above the melting temperature, were strong enough to keep the solid-like behavior (Fig. 6).

When the hydrogel with a specific initial shape is heated above the melting temperature of crystals, it can be deformed to a temporary shape by applying a convenient stress. The physical associations among alkyl chains act as crosslinking units enabling the strain of elastic chains and storing elastic energy in the material with the temporary shape. Cooling produces the freezing of the temporary shape by the crystallization of the aggregates of alkyl chains. When the stress is removed and the material is heated again above the melting temperature, elastic chains recover their initial configuration and the temporary shape is transformed to the initial one. Fig. 7 shows the 15 s recovery of a temporary compressed ring to the initial shape when heating at 60 °C. Hydrogels also exhibited self-healing ability (e.g., welding of two separate parts), above the melting temperature (24 h at 80 °C). This arises from the re-association process of alkyl chains at the interface.

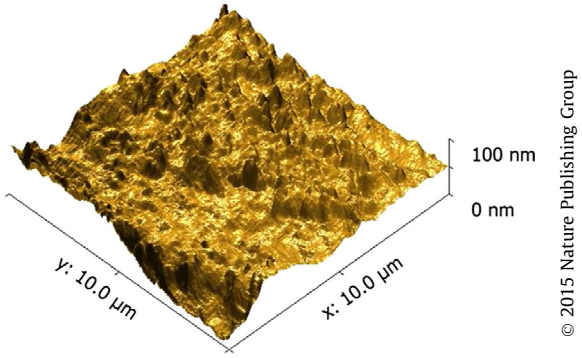

Fig. 5. Atomic Force Microscopy (AFM) image of the surface of the coating. Reprinted with permission from Ramakrishna et al. [25].

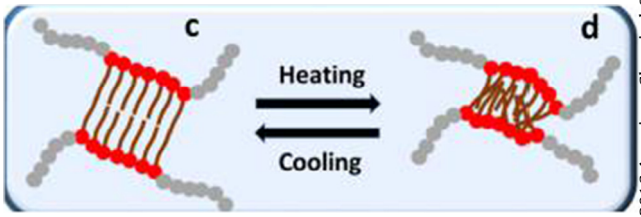

Fig. 6. Scheme of the hydrogel structure above the melting temperature and below the crystallization temperature of crystals formed by the tail-to-tail association of alkyl chains. Reprinted with permission from Bilici et al. [27].

Fig. 7. Recovery of a temporary compressed ring to the initial shape when heating at 60 °C. Reprinted with permission from Bilici et al. [27].

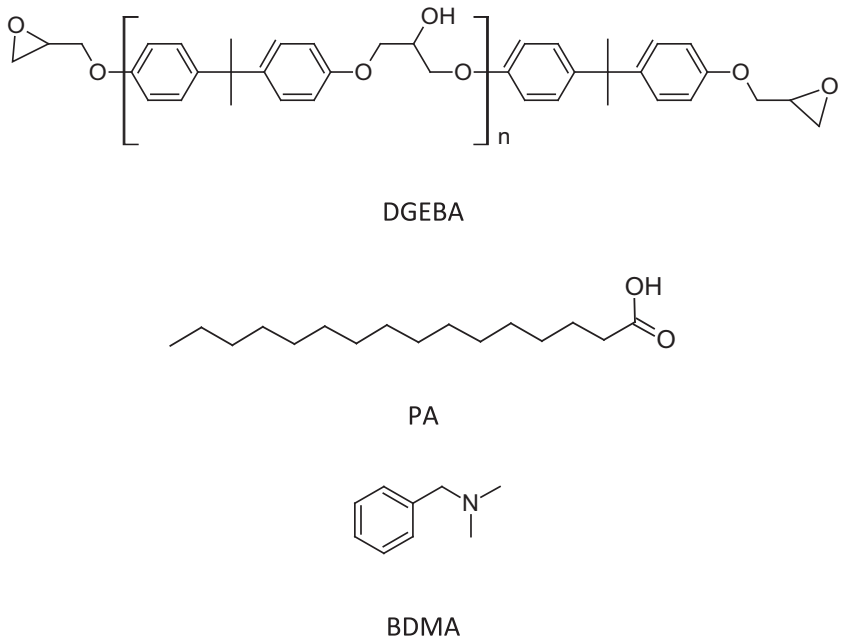

Fig. 8. Chemical structures of the epoxy monomer diglycidylether of bisphenol A (DGEBA), palmitic acid (PA) and benzyldimethylamine (BDMA).

3.3. Alkyl-modified epoxies as hot-melt adhesives

Epoxy networks obtained from a broad range of formulations dominate the field of adhesives. However, due to their crosslinked structure they cannot be employed as hot-melt adhesives. For this application, a crystallization process is needed such that the material behaves as a liquid above the melting temperature and becomes solid below the crystallization temperature while exhibiting good adhesive properties. The modification of a typical epoxy monomer with a fatty acid led to a convenient product for this application [32]. The formulation employed was based on the compounds shown in Fig. 8.

The tertiary amine (BDMA) acts as a catalyst for the epoxy-acid addition, generating a hydroxyester group bounded to the alkyl chain. Epoxy groups, used in excess with respect to acid groups, undergo homopolymerization initiated by the same tertiary amine after completion of the epoxy-acid reaction. The homopolymerization can give place to a gel or to a liquid, depending on the initial molar ratio of epoxy groups with respect to PA, E/PA. The critical gelation ratio was experimentally observed for E/PA = 3. Smaller values of E/PA led to a liquid phase at full conversion of epoxy groups. The liquid was formed by a distribution of branched oligomers with pendant alkyl chains. Crystallization of alkyl chains was observed when cooling the liquid to room temperature.

The fraction of (CH_2) units of alkyl chains that could be crystallized from liquids with different E/PA molar ratios was determined by differential scanning calorimetry (DSC). Results are shown in Fig. 9.

The fraction of crystallizable (CH_2) groups decreased almost linearly from about 54 % for E/PA = 1, to 14 % for E/PA = 2. The decrease in crystallinity may be associated to the generation of larger branched structures when approaching the critical gelation ratio, a fact that makes more difficult the alignment of alkyl chains in all-trans conformation needed to generate crystals. Melting temperatures decrease from 37 °C to 24 °C in the same range of molar ratios. This is a convenient temperature range for the application of these products as hot-melt adhesives.

Fig. 10 shows single lap-shear strength values of formulations with E/PA = 1.6, 1.8 and 2, employed as hot-melt adhesives. The product synthesized with E/PA = 2 exhibits a single lap-shear strength value of 2.5 MPa that lies in the range required for hot-melt adhesives.

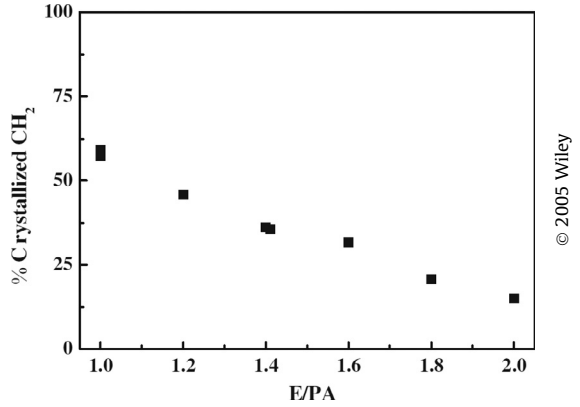

Fig. 9. Percent of (CH_2) groups of alkyl chains that crystallized for formulations with different E/PA molar ratios. Reprinted with permission from Hoppe et al. [32].

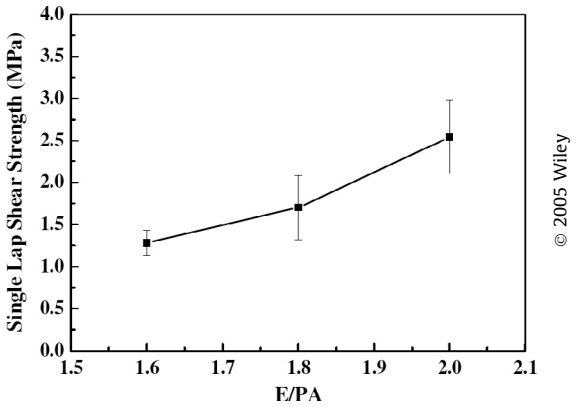

Fig. 10. Single lap-shear strength values of hot-melt adhesives synthesized with E/PA = 1.6, 1.8 and 2. Reprinted with permission from Hoppe et al. [32].

3.4. Thermally reversible light scattering (TRLS) films

TRLS films are used as coatings for the so-called intelligent windows, due to their capacity to change from an opaque to a transparent state above a particular temperature. One way to achieve this behavior is to employ a blend of a crystalline material with an amorphous polymer such that there is a matching of both refractive indices above the melting temperature. In this way, the blend is transparent at high temperatures but becomes opaque at low temperatures due to the light scattering produced by the crystals formed on cooling. However, in order to obtain a reversible behavior in a large number of heating/cooling cycles, it is necessary that the liquid formed when increasing temperature remains confined and does not leak, which usually requires the use of a thermally stable matrix and a suitable control of the morphology of the dispersion. This requirement can be fulfilled by selecting a crystalline modifier that simultaneously behaves as an organic gelator of a reactive solvent. The tridimensional structure formed during gelation allows obtaining a homogeneous distribution of crystals (responsible for scattering) and, at the same time, enables the immobilization of a reactive monomer that can then be polymerized, fixing the morphology in the desired way.

A TRLS film with excellent properties was generated from a blend of DGEBA capped at both ends by a fatty acid and a methacrylic monomer [31]. Stoichiometric amounts of stearic acid (SA, 2 mol) and DGEBA (1 mol) were reacted to full conversion. The structure of the resulting compound, DGEBA-$(SA)_2$, is shown in Fig. 11.

The crystallization and melting of DGEBA-$(SA)_2$ was analyzed by DSC. It crystallized below 40 °C and melted at 45 °C which is a convenient temperature range for its use as the crystalline component of a TRLS film. At relatively low concentrations in a particular solvent (THF, isopropanol, etc.) it loses solubility due to crystallization. However, instead of producing a precipitate, crystallization generates a gel due to the percolation of the crystalline structure throughout the material that encapsulates the solvent. Compounds synthesized in a similar way using other fatty acids exhibited the same behavior and make part of a new family of organogelators [31]. Percolation of the crystalline structure at low concentrations is possibly promoted by the rigidity of the DGEBA structure and the tail-to tail association of clusters of alkyl chains.

DGEBA-$(SA)_2$ was used as the crystalline component of a TRLS film. The other selected component was poly(ethylene glycol) dimethacrylate (PEGDMA, M_n = 550 g/mol, Fig. 11), due to the matching of refractive indices of the polymer network formed by polymerization of methacrylate groups and DGEBA-$(SA)_2$ in the amorphous phase. Both components were blended in the same mass amounts (50 wt%). Camphorquinone (CQ, Fig. 11) and ethyl-4-dimethyl aminobenzoato (EDMAB, Fig. 11) were employed for the photopolymerization of PEGDMA.

TRLS films were obtained by casting the blends between glass covers, using a steel spacer of 200 μm thickness. Irradiation was performed at room temperature with a light-emitting diode array (410–530 nm, 600 mW/cm^2) for two consecutive periods of 30 s. This led to a complete conversion of methacrylate groups.

Fig. 12a shows the optical transmittance as a function of temperature for the TRLS film subjected to a heating/cooling cycle at 20 °C/min. Above 48 °C the transmittance was close to 100 % due to the matching of refractive indices of both components. Below 37 °C, DGEBA-$(SA)_2$ crystallized and the transmittance dropped to about 35 %. As shown in Fig. 12b, at this transmission level the film appears as opaque. This behavior could be reproduced in several consecutive cycles and the optical contrast was not affected by the cooling rate.

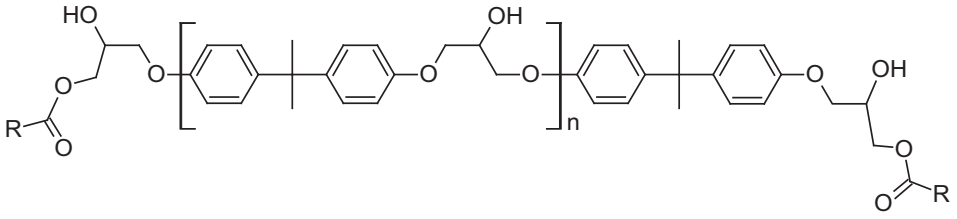

DGEBA-$(SA)_2$ R = -$(CH_2)_{16}$-CH_3

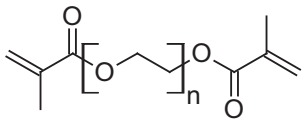

PEGDMA

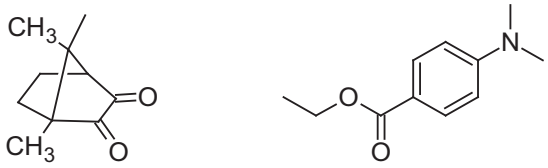

CQ EDMAB

Fig. 11. Chemical structures of DGEBA-$(SA)_2$, PEGDMA, CQ and EDMAB.

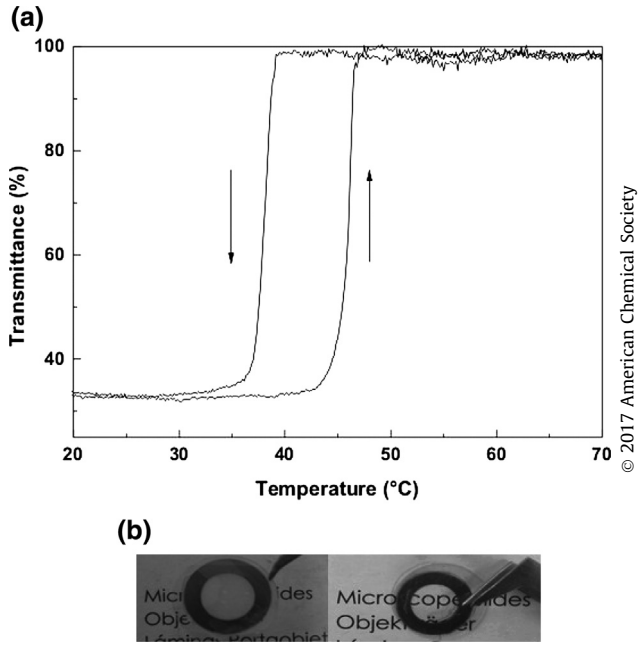

Fig. 12. (a) Optical transmittance as a function of temperature for the TRLS film subjected to a heating/cooling cycle at 20 °C/min; (b) Optical images of the TRLS film in the opaque (left) and transparent (right) states. Reprinted with permission from Puig et al. [31].

3.5. Form-Stable phase change materials (FS-PCMs) for thermal energy storage

PCMs absorb energy during melting and release energy during crystallization, a fact that is employed for different applications related to the absorption, storage and release of thermal energy. Among the large number of commercial compounds used as PCM, paraffins play a predominant role due to their outstanding properties like low cost, availability, large heats of crystallization/melting and chemical stability. For practical applications paraffins are encapsulated to prevent leakage during melting. This can be avoided if paraffins are part of a gel, generating a FS-PCM. For efficiency purposes, the requirement is to employ a low mass fraction of gel-forming material together with a large mass fraction of PCM. Organogelators formed by capping epoxy groups of DGEBA with stoichiometric amounts of a fatty acid may be useful for this purpose, provided that their melting temperatures are higher than the melting temperature of the paraffin so that the encapsulation is not destroyed during application.

An FS-PCM was synthesized using a DGEBA monomer end-capped with stoichiometric amounts of behenic acid (BA, Fig. 13), DGEBA-$(BA)_2$. [31] The melting temperature of DGEBA-$(BA)_2$ is 62 °C which is the limiting operation temperature for its use as encapsulant of a PCM. Eicosane (Fig. 13) with a melting temperature of 37 °C was employed as PCM. The FS-PCM was obtained by blending both components (80 wt% eicosane in the blend) at temperatures above the melting temperature of the organogelator and cooling to room temperature.

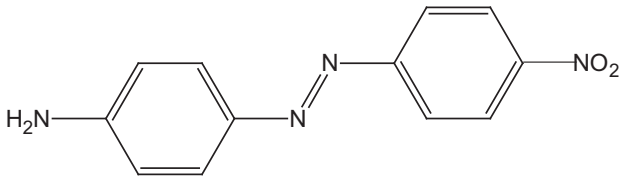

Fig. 14. Chemical structure of Disperse Orange-3.

The FS-PCM exhibited an excellent performance for the storage of thermal energy. The heat absorbed during the melting of encapsulated eicosane was 161 J/g as determined by DSC scans. This corresponds to a fraction of crystallized eicosane close to 81 % meaning that encapsulation did not produce a significant loss of crystallinity.

4. Advanced materials based on amorphous associations of alkyl chains in the bulk

The crystallization of alkyl chains within a material depends on several parameters like chain length, steric impediment for crystallization, nature of the surrounding environment, etc. Hence, hydrophobic association among alkyl chains not necessarily led to the formation of crystalline domains. Nevertheless, non-crystalline domains formed by self-assembly of alkyl chains (ordered or disordered), have proved to be very valuable for the synthesis of amphiphilic networks [35,36], supramolecular objects [37,38], liquid crystalline systems [39,40], shape memory polymers [15], self-healing materials [41], etc. In order to show the huge potentiality that arises from the rational use of these materials, in this section we focus the discussion on new materials that combine self-association of alkyl chains in amorphous domains with a specific functionality derived from the inclusion of a nanostructure or an optically active molecule (azobenzene).

4.1. Materials with reversible optical storage

Irradiating a glassy material containing azobenzene moieties with linearly polarized light leads to the buildup of photoinduced anisotropy due to the trans-cis isomerization of azobenzene groups. The initially isotropic material becomes birefringent. However, when irradiation ceases a partial relaxation of the orientation takes place leading to a constant remnant birefringence. Irradiation with circularly polarized light brings back the material to the initial random distribution of azoisomers [42].

A linear epoxy polymer containing azobenzene moieties was obtained by reaction of DGEBA with a blend of two monoamines: dodecylamine (DA) and an azobenzene containing amine (Disperse

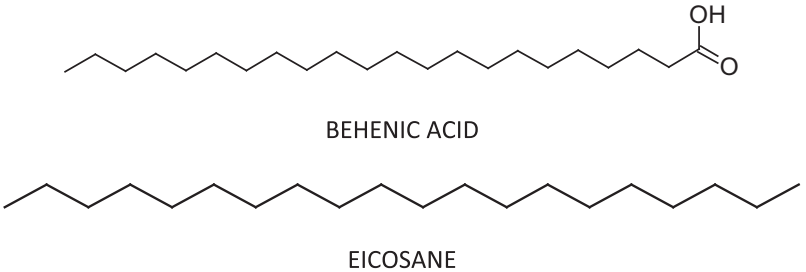

Fig. 13. Chemical structures of behenic acid (BA) and eicosane.

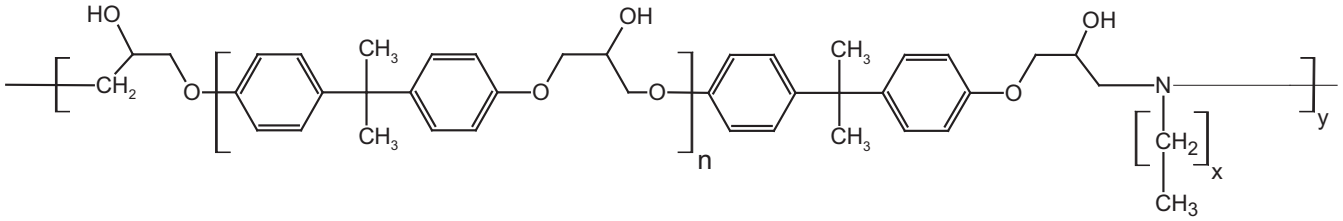

Fig. 15. Chemical structure of the repeating unit of the linear polymer produced by reaction of stoichiometric amounts of DGEBA and an *n*-alkylamine.

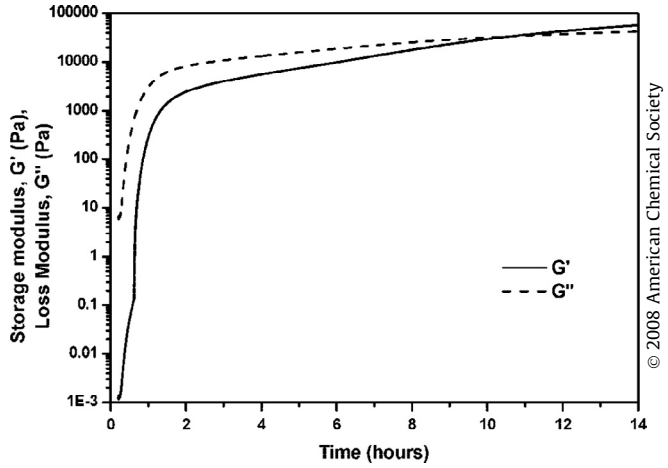

Fig. 16. Evolution of the storage (G') and loss moduli (G'') during reaction of stoichiometric amounts of DGEBA and DA at 100 °C. Reprinted with permission from Zucchi et al. [43].

Orange-3, DO3, chemical structure in Fig. 14). The sum of DA and DO3 was stoichiometric with respect to DGEBA. As both amine hydrogens react with epoxy groups, the reaction product is a linear polymer containing pendant alkyl and azobenzene groups distributed along the chain.

Optical properties of one of the materials reported in Ref. [42] will be discussed. This material was synthesized employing a molar ratio DO3/DA = 3. In order to enhance the associations among pendant alkyl chains, the reaction was carried out in two steps. First, DGEBA and DA were reacted for 1 h at 100 °C in the corresponding epoxy excess. This led to relatively short oligomers terminated in epoxy groups. Then, DO3 was added and its reaction with residual epoxy groups was performed at 180 °C. This led to multiblock linear chains containing short $(DGEBA\text{-}DA)_n$ blocks and large $(DGEBA\text{-}DO3)_m$ blocks [42].

Associations among alkyl chains could be enhanced by annealing the linear polymer at 60 °C for 24 h. The generated crosslinks increased the glass transition temperature from 34 °C before annealing to 56 °C after annealing. The physical crosslinks also produced an increase in birefringence from 0.025 to 0.032 and in the percent of remnant birefringence from 37 to 58 % [42].

4.2. Photoluminescent nanocomposites

CdSe quantum dots (QD) nanocrystals stabilized by hydrophobic ligands can be employed to generate fluorescent nanocomposites. The matrix employed to produce a uniform dispersion of these NPs must be also hydrophobic or, alternatively, it should contain hydrophobic nanodomains. A comb-like polymer with pendant alkyl chains could be used for this purpose.

Linear amphiphilic polymers can be synthesized using stoichiometric amounts of DGEBA and *n*-alkylamines [36,43]. These polymers have a polar backbone with equally-spaced pendant alkyl chains. The chemical structure of the repeating unit is shown in Fig. 15.

Fig. 16 shows the evolution of the storage (G') and loss (G'') moduli during reaction of stoichiometric amounts of DGEBA and dodecylamine (DA), at 100 °C. When both components were blended at 100 °C, a micellar dispersion of the amphiphilic amine in the polar epoxy monomer was generated. The sudden increase of the storage modulus at about 1 h reaction was assigned to a phase inversion due to the partial depletion of the epoxy monomer. At this time, the continuous phase changed from the epoxy monomer to the generated comb-like polymer chains, partially in contact with other chains through tail-to-tail alkyl associations. Most of the epoxy conversion took place during the first 1–2 h. However, the storage modulus continued increasing together with the con-

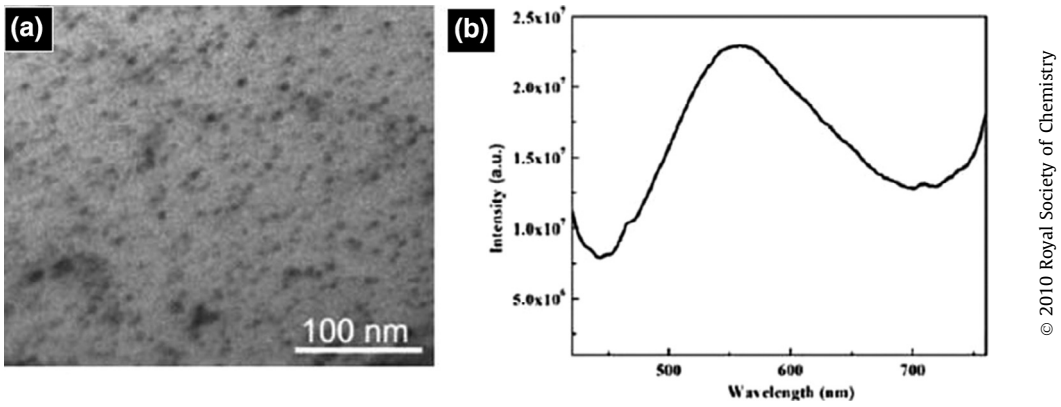

Fig.17. (a) TEM image of a slice of the physical gel infused by QD; (b) emission spectra obtained with an excitation length of 400 nm. Reprinted with permission from Ledo-Suárez et al. [44].

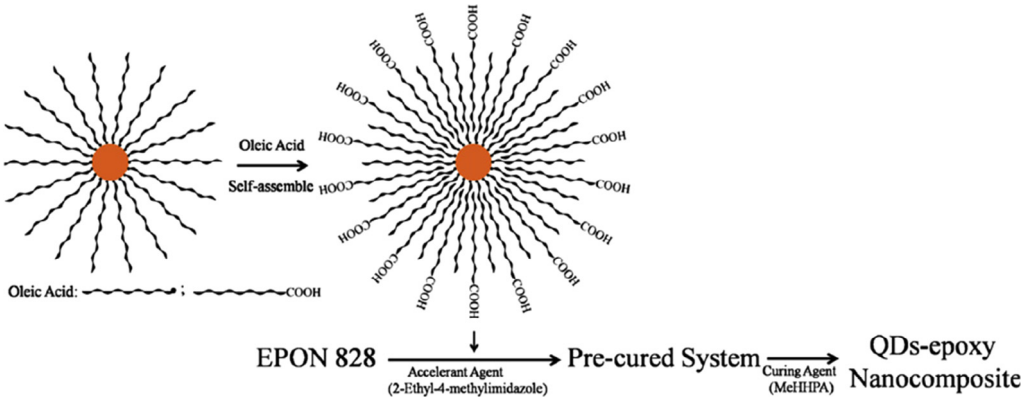

Fig. 18. Scheme of the functionalization of QD with carboxyl groups. Reprinted with permission from Zou et al. [45].

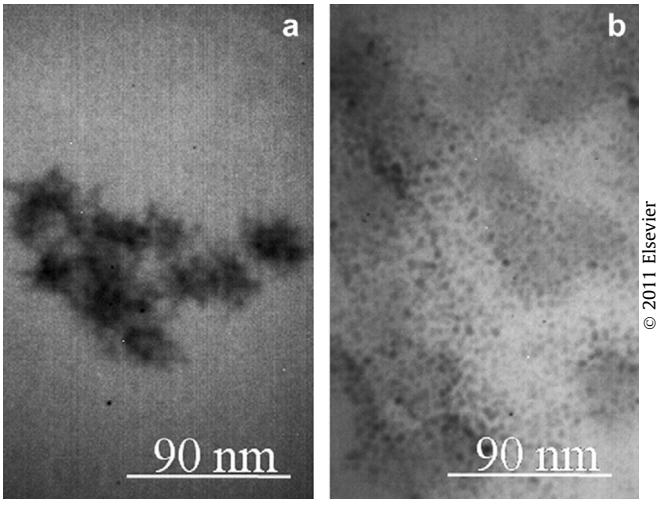

Fig. 19. TEM images of the dispersion of QD in the epoxy matrix. (a) Unmodified QD; (b) QD with inserted oleic acid chains. Reprinted with permission from Zou et al. [45].

centration of crosslinks produced by the association of alkyl chains. After about 10 h, the material gelled (G' surpassed G''). After about 14 h, the physical association of alkyl chains was almost complete.

When the material was cooled to room temperature and reheated, it was converted again to a liquid at about 160 °C, due to the thermal reversibility of the association of alkyl chains (weak gel to liquid transition). When the material previously heated to the liquid state was annealed at a lower temperature, physical associations of alkyl chains were produced leading again to a gel.

The gel employed to host the dispersion of QD stabilized with hydrophobic ligands was synthesized by reacting stoichiometric amounts of DGEBA and DA for 3 h at 100 °C, followed by annealing at 60 °C for 21 h. The last step was used to increase the concentration of physical crosslinks produced by association of alkyl chains. CdSe QD (3-nm average size) were dispersed in 1-octadecene/tetrahydrofuran, THF (50:50) and infused into the physical gel by immersion in the solution at room temperature for 24 h [44]. The change in color of the gel indicated successful infusion of NPs.

Fig. 17a shows a TEM image of a slice of the gel infused by QD. A uniform dispersion of NPs is observed with some clustering also revealed by the broad emission peak (Fig. 17b).

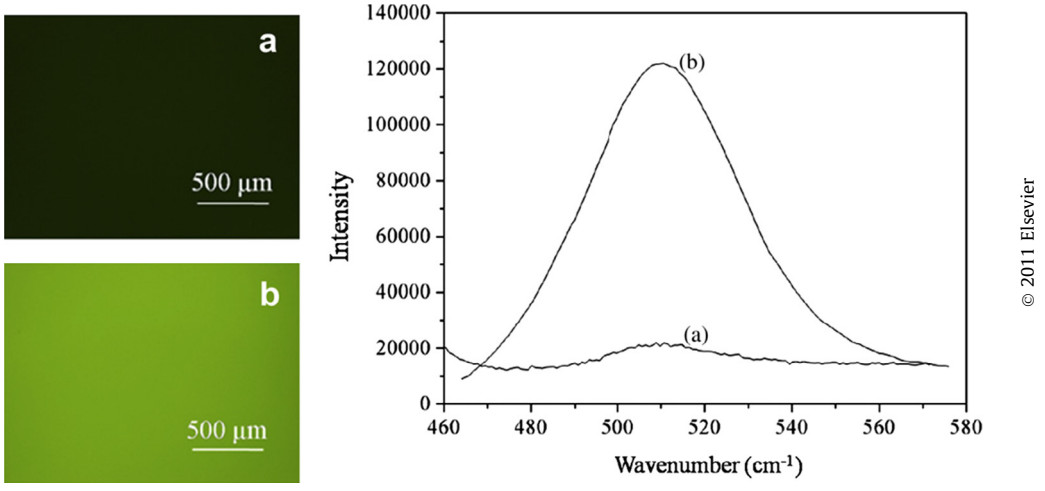

Fig. 20. Fluorescent microscope images and emission spectra of unmodified QD (a) and QD with inserted oleic acid chains (b), dispersed in the epoxy matrix. Reprinted with permission from Zou et al. [45].

A different strategy used to disperse CdSe QD in a polar epoxy matrix, was reported by Zou et al. [45]. CdSe QD were synthesized using oleic acid as the stabilizing ligand. Carboxyl groups remain at the surface of CdSe nanocrystals and the alkyl chains extend outside, as depicted in Fig. 18. When these NPs were dispersed in an oleic acid solution in THF, alkyl chains of oleic acid were inserted and self-assembled in the shell of stabilizing ligands, with the carboxyl groups located in the external surface in contact with the polar THF solvent (Fig. 18). This simple strategy enabled the functionalization of QD with carboxyl groups.

Carboxyl groups were then pre-reacted with DGEBA using a tertiary amine as catalyst and the polymer network was produced by adding an anhydride as hardener [45]. This led to a uniform dispersion of QD in the epoxy matrix. Fig. 19a is a TEM image of the dispersion of unmodified QD in the epoxy matrix showing large agglomerations of NPs. Fig. 19b shows the corresponding image for the dispersion of QD with inserted oleic acid chains. Now, a uniform dispersion of NPs is observed.

Fig. 20 shows fluorescent microscope images and emission spectra of QD-epoxy nanocomposites excited at 450 nm. In the case of unmodified QD, the large aggregation of NPs caused the quenching of the emission while for QD with inserted oleic acid chains, the typical emission band was observed. It is interesting to note that this result was simply obtained by enabling the physical association of functionalized alkyl chains with the alkyl chains employed as stabilizing ligands of the NPs. This opens an efficient and simple way to change the compatibility of alkyl chains used as standard ligands in a variety of methods employed for the synthesis of NPs.

5. Conclusions

The self-assembly of alkyl chains at an interface (like in SAMs) or at the bulk of a material (e.g. in comb-like polymers with pendant alkyl chains) has been deeply investigated for several decades. This natural property of alkyl chains has been employed in recent years to develop a new generation of materials for technological applications. The purpose of this article was to discuss some selected examples where the advanced properties arise from a process involving the self-assembly of alkyl chains. We included a description of electronic devices and new-generation catalysts where properties derived from a controlled 2D or 3D self-assembly of alkyl chains at an interface. Then, we showed that controlling the crystallization of alkyl chains at the bulk can be used to generate a variety of advanced materials such as superhydrophobic coatings, shape memory hydrogels, hot-melt adhesives, TRLS films for intelligent windows and FS-PCMs for the storage of thermal energy. Finally, we discussed two examples where advanced properties derive from the formation of disordered domains by physical association of alkyl chains. This was the case of materials used for reversible optical storage and of photoluminescent nanocomposites. These examples are just a sub-set of many others that may be found in the literature and that include applications spanning areas as diverse as tribology, energy harvesting or micro and nano-fabrication. However, they are enough to illustrate how advanced properties can be generated by conveying the natural self-assembly process of alkyl chains in a convenient way. No complex synthesis was required in any of these cases. Commercial compounds were employed and one-step simple chemical reactions were used when required. We hope that these examples can encourage the use of the self-assembly of alkyl chains to develop a new generation of advanced materials.

Acknowledgements

The financial support of the following institutions is gratefully acknowledged: National Research Council (CONICET, PIP N° 0594), National Agency for the Promotion of Science and Technology (ANPCyT, Argentina, PICT015-1433, PICT012-2235 and PICT10-1008) and University of Mar del Plata (15/G374).

References

[1] M.D. Porter, T.B. Bright, D.L. Allara, C.E.D. Chidsey, Spontaneously organized molecular assemblies. 4. Structural characterization of n-alkyl thiol monolayers on gold by optical ellipsometry, infrared spectroscopy, and electrochemistry, J. Am. Chem. Soc. 109 (1987) 3559–3568, https://doi.org/10.1021/ja00246a011.
[2] J.C. Love, L.A. Estroff, J.K. Kriebel, R.G. Nuzzo, G.M. Whitesides, Self-assembled monolayers of thiolates on metals as a form of nanotechnology, Chem. Rev. 105 (2005) 1103–1170, https://doi.org/10.1021/cr0300789.
[3] N.A. Platé, V.P. Shibaev, Comb-like polymers. Structure and properties, J. Polym. Sci. Macromol. Rev 8 (1974) 117–253, https://doi.org/10.1002/pol.1974.230080103.
[4] T. Babur, G. Gupta, M. Beiner, About different packing states of alkyl groups in comb-like polymers with rigid backbones, Soft Matter. 12 (2016) 8093–8097, https://doi.org/10.1039/C6SM01812B.
[5] R. Phillipson, C.J. Lockhart de la Rosa, J. Teyssandier, P. Walke, D. Waghray, Y. Fujita, J. Adisoejoso, K.S. Mali, I. Asselberghs, C. Huyghebaert, H. Uji-i, S. De Gendt, S. De Feyter, Tunable doping of graphene by using physisorbed self-assembled networks, Nanoscale 8 (2016) 20017–20026, https://doi.org/10.1039/C6NR07912A.
[6] R.L. Whetten, M.N. Shafigullin, J.T. Khoury, T.G. Schaaff, I. Vezmar, M.M. Alvarez, A. Wilkinson, Crystal structures of molecular gold nanocrystal arrays, Acc. Chem. Res. 32 (1999) 397–406, https://doi.org/10.1021/ar970239t.
[7] W.D. Luedtke, U. Landman, Structure, dynamics, and thermodynamics of passivated gold nanocrystallites and their assemblies, J. Phys. Chem. 100 (1996) 13323–13329, https://doi.org/10.1021/jp961721g.
[8] M.P. Pileni, ed., Nanocrystals forming mesoscopic structures, Wiley-VCH ; John Wiley [distributor], Weinheim : Chichester, 2005.
[9] M. Beiner, H. Huth, Nanophase separation and hindered glass transition in side-chain polymers, Nat. Mater. 2 (2003) 595–599, https://doi.org/10.1038/nmat966.
[10] X. Chen, N. Zheng, Q. Wang, L. Liu, Y. Men, Side-chain crystallization in alkyl-substituted cellulose esters and hydroxypropyl cellulose esters, Carbohydr. Polym. 162 (2017) 28–34, https://doi.org/10.1016/j.carbpol.2017.01.028.
[11] S.-H. Cha, J.-U. Kim, K.-H. Kim, J.-C. Lee, Preparation and photoluminescent properties of gold(I)–alkanethiolate complexes having highly ordered supramolecular structures, Chem. Mater. 19 (2007) 6297–6303, https://doi.org/10.1021/cm7024944.
[12] A. Shimojima, K. Kuroda, Designed synthesis of nanostructured siloxane–organic hybrids from amphiphilic silicon-based precursors, Chem. Rec. 6 (2006) 53–63, https://doi.org/10.1002/tcr.20073.
[13] A.A. Hiwale, C. Voshavar, P. Dharmalingam, A. Dhayani, R. Mukthavaram, R. Nadella, O. Sunnapu, S. Gandhi, V.G.M. Naidu, A. Chaudhuri, S. Marepally, P.K. Vemula, Scaling the effect of hydrophobic chain length on gene transfer properties of di-alkyl, di-hydroxy ethylammonium chloride based cationic amphiphiles, RSC Adv. 7 (2017) 25398–25405, https://doi.org/10.1039/C7RA02271A.
[14] S.K. Pathak, B. Pradhan, M. Gupta, S.K. Pal, A.A. Sudhakar, Liquid-crystalline star-shaped supergelator exhibiting aggregation-induced blue light emission, Langmuir. 32 (2016) 9301–9312, https://doi.org/10.1021/acs.langmuir.6b02509.
[15] K. Inomata, T. Terahama, R. Sekoguchi, T. Ito, H. Sugimoto, E. Nakanishi, Shape memory properties of polypeptide hydrogels having hydrophobic alkyl side chains, Polymer. 53 (2012) 3281–3286, https://doi.org/10.1016/j.polymer.2012.05.036.
[16] E. Harputlu, K. Ocakoglu, F. Yakuphanoglu, A. Tarnowska, D.T. Gryko, Physical properties of self-assembled zinc chlorin nanowires for artificial light-harvesting materials, Nano-Struct. Nano-Objects. 10 (2017) 9–14, https://doi.org/10.1016/j.nanoso.2017.02.002.
[17] J. Hühn, C. Carrillo-Carrion, M.G. Soliman, C. Pfeiffer, D. Valdeperez, A. Masood, I. Chakraborty, L. Zhu, M. Gallego, Z. Yue, M. Carril, N. Feliu, A. Escudero, A.M. Alkilany, B. Pelaz, P. del Pino, W.J. Parak, Selected standard protocols for the synthesis, phase transfer, and characterization of inorganic colloidal nanoparticles, Chem. Mater. 29 (2017) 399–461, https://doi.org/10.1021/acs.chemmater.6b04738.
[18] M.A. Boles, M. Engel, D.V. Talapin, Self-assembly of colloidal nanocrystals: from intricate structures to functional materials, Chem. Rev. 116 (2016) 11220–11289, https://doi.org/10.1021/acs.chemrev.6b00196.
[19] A.M. Shanmugharaj, J.H. Yoon, W.J. Yang, S.H. Ryu, Synthesis, characterization, and surface wettability properties of amine functionalized graphene oxide films with varying amine chain lengths, J. Colloid Interface Sci. 401 (2013) 148–154, https://doi.org/10.1016/j.jcis.2013.02.054.

[20] Y. Kim, J. Ryu, M. Park, E.S. Kim, J.M. Yoo, J. Park, J.H. Kang, B.H. Hong, Vapor-phase molecular doping of graphene for high-performance transparent electrodes, ACS Nano. 8 (2014) 868–874, https://doi.org/10.1021/nn405596j.
[21] P.T. Witte, S. Boland, F. Kirby, R. van Maanen, B.F. Bleeker, D.A.M. de Winter, J. A. Post, J.W. Geus, P.H. Berben, NanoSelect Pd catalysts: what causes the high selectivity of these supported colloidal catalysts in alkyne semi-hydrogenation?, ChemCatChem 5 (2013) 582–587, https://doi.org/10.1002/cctc.201200460.
[22] P.T. Witte, P.H. Berben, S. Boland, E.H. Boymans, D. Vogt, J.W. Geus, J.G. Donkervoort, B.A.S.F. NanoSelectTM Technology, Innovative supported Pd- and Pt-based catalysts for selective hydrogenation reactions, Top. Catal. 55 (2012) 505–511, https://doi.org/10.1007/s11244-012-9818-y.
[23] D. Albani, G. Vilé, S. Mitchell, P.T. Witte, N. Almora-Barrios, R. Verel, N. López, J. Pérez-Ramírez, Ligand ordering determines the catalytic response of hybrid palladium nanoparticles in hydrogenation, Catal Sci Technol. 6 (2016) 1621–1631, https://doi.org/10.1039/C5CY01921D.
[24] K. Nakano, S. Akita, M. Yamanaka, Fabrication of superhydrophobic surfaces from mixtures of aluminum distearate and fatty acids via intermediate organogel formation, Colloid Polym. Sci. 292 (2014) 1475–1478, https://doi.org/10.1007/s00396-014-3219-7.
[25] S. Ramakrishna, K.S. Santhosh Kumar, D. Mathew, C.P. Reghunadhan Nair, A robust, melting class bulk superhydrophobic material with heat-healing and self-cleaning properties, Sci. Rep. 5 (2015) 18510, https://doi.org/10.1038/srep18510.
[26] D. Wu, W. Wen, S. Chen, H. Zhang, Preparation and properties of a novel form-stable phase change material based on a gelator, J. Mater. Chem. A. 3 (2015) 2589–2600, https://doi.org/10.1039/C4TA06508E.
[27] C. Bilici, V. Can, U. Nöchel, M. Behl, A. Lendlein, O. Okay, Melt-processable shape-memory hydrogels with self-healing ability of high mechanical strength, Macromolecules. 49 (2016) 7442–7449, https://doi.org/10.1021/acs.macromol.6b01539.
[28] D. Pei, S. Chen, S. Li, H. Shi, W. Li, X. Li, X. Zhang, Fabrication and properties of poly(polyethylene glycol n-alkyl ether vinyl ether)s as polymeric phase change materials, Thermochim. Acta. 633 (2016) 161–169, https://doi.org/10.1016/j.tca.2016.04.007.
[29] B. Kurt, U. Gulyuz, D.D. Demir, O. Okay, High-strength semi-crystalline hydrogels with self-healing and shape memory functions, Eur. Polym. J. 81 (2016) 12–23, https://doi.org/10.1016/j.eurpolymj.2016.05.019.
[30] V. Schimpf, B. Heck, G. Reiter, R. Mülhaupt, Triple-shape memory materials via thermoresponsive behavior of nanocrystalline non-isocyanate polyhydroxyurethanes, Macromolecules. 50 (2017) 3598–3606, https://doi.org/10.1021/acs.macromol.7b00500.
[31] J. Puig, I.E. dell' Erba, W.F. Schroeder, C.E. Hoppe, R.J.J. Williams, Epoxy-based organogels for thermally reversible light scattering films and form-stable phase change materials, ACS Appl. Mater. Interfaces. 9 (2017) 11126–11133, https://doi.org/10.1021/acsami.7b00086.
[32] C.E. Hoppe, M.J. Galante, P.A. Oyanguren, R.J.J. Williams, Epoxies modified by palmitic acid: from hot-melt adhesives to plasticized networks, Macromol. Mater. Eng. 290 (2005) 456–462, https://doi.org/10.1002/mame.200400348.
[33] S. Gu, L. Duan, X. Ren, G.H. Gao, Robust, tough and anti-fatigue cationic latex composite hydrogels based on dual physically cross-linked networks, J. Colloid Interface Sci. 492 (2017) 119–126, https://doi.org/10.1016/j.jcis.2017.01.002.
[34] C. Bilici, O. Okay, Shape memory hydrogels via micellar copolymerization of acrylic acid and *n* -octadecyl acrylate in aqueous media, Macromolecules. 46 (2013) 3125–3131, https://doi.org/10.1021/ma400494n.
[35] J.P. Pascault, R.J.J. Williams (Eds.), Epoxy polymers: new materials and innovations, Wiley-VCH, Weinheim, 2010.
[36] J. Puig, I.A. Zucchi, C.E. Hoppe, C.J. Pérez, M.J. Galante, R.J.J. Williams, C. Rodríguez-Abreu, Epoxy networks with physical cross-links produced by tail-to-tail associations of alkyl Chains, Macromolecules. 42 (2009) 9344–9350, https://doi.org/10.1021/ma9018203.
[37] P. Chidchob, T.G.W. Edwardson, C.J. Serpell, H.F. Sleiman, Synergy of two assembly languages in DNA nanostructures: self-assembly of sequence-defined polymers on DNA cages, J. Am. Chem. Soc. 138 (2016) 4416–4425, https://doi.org/10.1021/jacs.5b12953.
[38] S. Shoji, T. Hashishin, H. Tamiaki, Construction of chlorosomal rod self-aggregates in the solid state on any substrates from synthetic chlorophyll derivatives possessing an oligomethylene chain at the 17-propionate residue, Chem. - Eur. J. 18 (2012) 13331–13341, https://doi.org/10.1002/chem.201201935.
[39] Y. Xiao, H. Gao, T. Wang, R. Zhang, X. Cheng, Synthesis, liquid-crystalline, photophysical and chemosensor properties of oxadiazole/thiadiazole-based amphiphiles with glycerol groups, J. Mol. Liq. 244 (2017) 360–367, https://doi.org/10.1016/j.molliq.2017.08.110.
[40] Y. Ren, R. Zhang, C. Yan, T. Wang, H. Cheng, X. Cheng, Self-assembly AIEE and mechanochromic properties of amphiphilic α-cyanostilbene derivatives, Tetrahedron. 73 (2017) 5253–5259, https://doi.org/10.1016/j.tet.2017.07.010.
[41] S. Seiffert, M. Anthamatten (Eds.), Supramolecular polymer networks and gels, Springer, Cham, 2015.
[42] M. Victorel, L.M. Sáiz, M.J. Galante, P.A. Oyanguren, Effects of physical crosslinks on the photoresponse of epoxy-based polymers, Eur. Polym. J. 76 (2016) 256–265, https://doi.org/10.1016/j.eurpolymj.2016.02.002.
[43] I.A. Zucchi, C.E. Hoppe, M.J. Galante, R.J.J. Williams, M.A. López-Quintela, L. Matějka, M. Slouf, J. Pleštil, Self-assembly of gold nanoparticles as colloidal crystals induced by polymerization of amphiphilic monomers, Macromolecules 41 (2008) 4895–4903, https://doi.org/10.1021/ma800457w.
[44] A. Ledo-Suárez, J. Puig, I.A. Zucchi, C.E. Hoppe, M.L. Gómez, R. Zysler, C. Ramos, M.C. Marchi, S.A. Bilmes, M. Lazzari, M.A. López-Quintela, R.J.J. Williams, Functional nanocomposites based on the infusion or in situ generation of nanoparticles into amphiphilic epoxy gels, J. Mater. Chem. 20 (2010) 10135–10145, https://doi.org/10.1039/c0jm01421d.
[45] W. Zou, Z. Du, H. Li, C. Zhang, Fabrication of carboxyl functionalized CdSe quantum dots via ligands self-assembly and CdSe/epoxy fluorescence nanocomposites, Polymer 52 (2011) 1938–1943, https://doi.org/10.1016/j.polymer.2011.02.043.